Available online at www.sciencedirect.com

SCIENCE DIRECT®

Experimental Cell Research 312 (2006) 256 – 265

Experimental Cell Research

www.elsevier.com/locate/yexcr

Research Article

Histone deacetylase inhibitor FR901228 enhances the antitumor effect of telomerase-specific replication-selective adenoviral agent OBP-301 in human lung cancer cells

Takanori Watanabe[a], Masayoshi Hioki[a], Toshiya Fujiwara[a], Masahiko Nishizaki[a], Shunsuke Kagawa[a,b], Masaki Taki[a], Hiroyuki Kishimoto[a], Yoshikatsu Endo[a], Yasuo Urata[c], Noriaki Tanaka[a], Toshiyoshi Fujiwara[a,b,*]

[a]*Division of Surgical Oncology, Department of Surgery, Okayama University, Graduate School of Medicine and Dentistry, Okayama, Japan*
[b]*Center for Gene and Cell Therapy, Okayama University Hospital, Okayama, Japan*
[c]*Oncolys BioPharma, Inc., Tokyo, Japan*

Received 9 June 2005, revised version received 17 October 2005, accepted 21 October 2005

Abstract

Replication-competent oncolytic viruses are being developed for human cancer therapy. We previously reported that an attenuated adenovirus OBP-301 (Telomelysin), in which the human telomerase reverse transcriptase promoter element drives expression of E1A and E1B genes linked with an internal ribosome entry site, could replicate in and causes selective lysis of human cancer cells. Infection efficiency in target cancer cells is the most important factor that predicts the antitumor effects of OBP-301. The objectives of this study are to examine the effects of the histone deacetylase inhibitor FR901228 on the level of coxsackie and adenovirus receptor (CAR) expression and OBP-301-mediated oncolysis in human non-small cell lung cancer cell lines. Flow cytometric analysis revealed up-regulated CAR expression in A549 and H460 cells following treatment with 1 ng/ml of FR901228, which was associated with increased infection efficiency as confirmed by replication-deficient β-galactosidase-expressing adenovirus vector. In contrast, neither CAR expression nor infection efficiency was affected by FR901228 in H1299 cells. To visualize and quantify viral replication in the presence of FR901228, we used OBP-401 (Telomelysin-GFP) that expresses the green fluorescent protein (GFP) reporter gene under the control of the cytomegalovirus promoter in the E3 region. Fluorescence microscopy and flow cytometry showed that FR901228 increased GFP expression in A549 and H460 cells following OBP-401 infection in a dose-dependent manner, but this effect did not occur in H1299 cells. In addition, OBP-301 and FR901228 demonstrated a synergistic antitumor effect in A549 cells in vitro, as confirmed by isobologram analysis. Our data indicate that FR901228 preferentially increases adenovirus infectivity via up-regulation of CAR expression, leading to a profound oncolytic effect, which may have a significant impact on the outcome of adenovirus-based oncolytic virotherapy.

Keywords: Oncolytic virus; HDAC inhibitor; Adenovirus; CAR; Lung cancer

Introduction

Replication-selective, oncolytic viruses provide a new platform to treat a variety of human cancers [1,2]. Promising clinical trial data have shown the antitumor potency and safety of mutant or genetically modified adenoviruses [3–6]. We previously constructed an adenovirus vector (OBP-301, Telomelysin), in which the human telomerase reverse transcriptase (hTERT) promoter element drives expression of E1A and E1B genes linked with an internal ribosome entry site (IRES). We showed that OBP-301 caused efficient selective killing in human cancer cells, but not in normal cells [7]. Although OBP-301 demonstrated a broad-spec-

* Corresponding author. Center for Gene and Cell Therapy, Okayama University Hospital, 2-5-1 Shikata-cho, Okayama 700-8558, Japan. Fax: +81 86 235 7884.
E-mail address: toshi_f@md.okayama-u.ac.jp (T. Fujiwara).

0014-4827/$ - see front matter © 2005 Elsevier Inc. All rights reserved.
doi:10.1016/j.yexcr.2005.10.026

trum antitumor activity, infection efficiency of the presently available adenoviral agent, which is derived from human adenovirus serotype 5, varies widely depending on the expression of coxsackie-adenovirus receptor (CAR) [8,9]. To overcome the limitation of low levels of CAR in certain tumors, we further modified the fiber of OBP-301 to contain RGD peptide. We demonstrated that this fiber-modified OBP-405 permits CAR-independent cell entry and effective destruction of tumors lacking the primary CAR [10]. This strategy has been commonly used to alter adenovirus infectivity [11,12]; the genetic modification, however, might not always be successful. An alternative approach is to modify CAR expression in target tumor cells.

FR901228 (Depsipeptide, FK228) is a novel anticancer agent isolated from the fermentation broth of *Chromobacterium violaceum*. FR901228 has been identified as a potent histone deacetylase (HDAC) inhibitor, although it has no apparent chemical structure that interacts with the HDAC

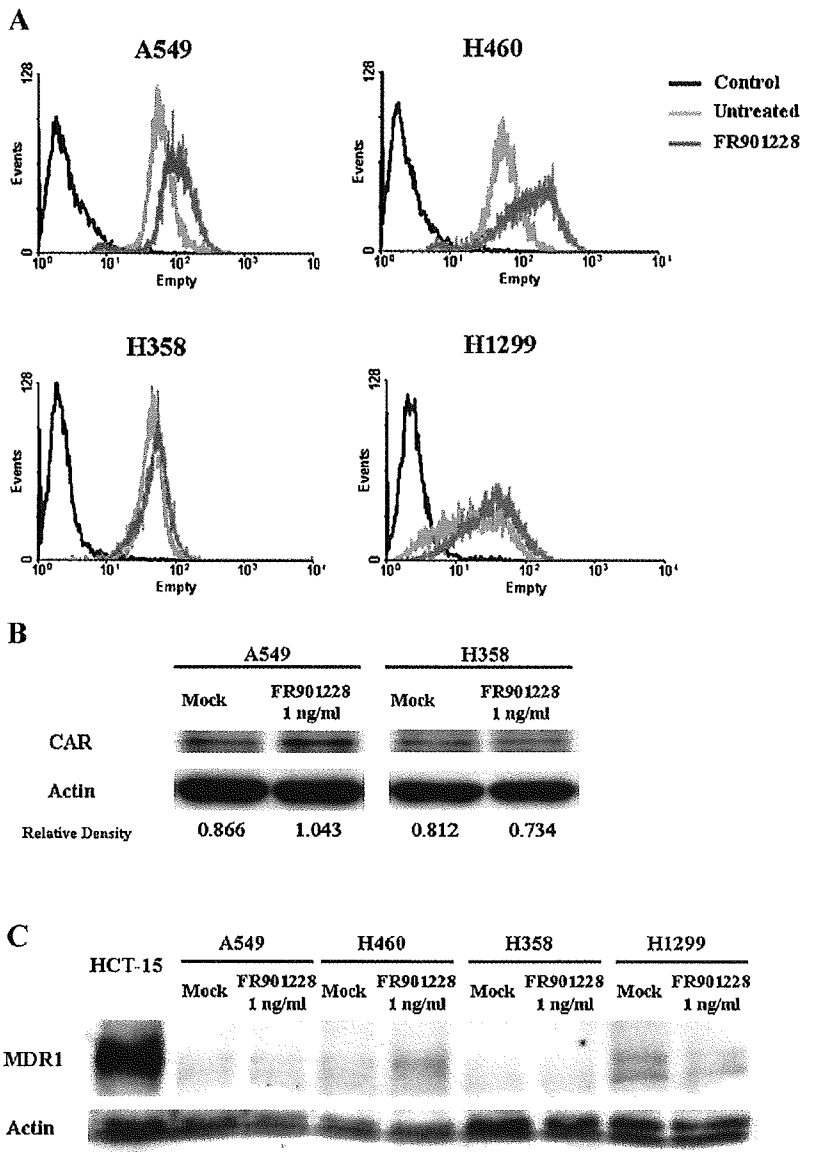

Fig. 1. (A) Expression of CAR on human NSCLC cell lines after FR901228 treatment. Cells were treated with 1 ng/ml of FR901228 for 48 h and then subjected to flow cytometric analysis. Both treated and untreated cells were incubated with mouse monoclonal anti-CAR (RmcB) followed by detection with FITC-labeled secondary antibody. An isotype-matched normal mouse IgG1 conjugated to FITC was used as a control in all experiments. The rightward shift of the histogram after exposure to FR901228 indicates increased CAR expression. (B) Western blot analysis of CAR and actin in A549 and H358 cells. Cells were treated same as above. Equivalent amounts of protein obtained from whole cell lysates were loaded in each lane, probed with anti-CAR antibody, and then visualized by using an ECL detection system. Equal loading of samples was confirmed by stripping each blot and reprobing with anti-actin antiserum. CAR protein expression was quantified by densitometric scanning using NIH Image software and normalization by dividing the actin signal. (C) Western blot analysis for MDR1 expression. Equivalent amounts of protein obtained from whole cell lysates were loaded in each lane and probed with anti-MDR1 antibody with or without FR901228 treatment. The cell lysate obtained from HCT-15 human colorectal cancer cells was used as a positive control.

active-site pocket. Thus, FR901228 is structurally distinct from other known HDAC inhibitors such as the trichostatins and trapoxins [13–15]. Histone deacetylation is an important component of transcriptional control, and it has been reported that FR901228 can increase CAR gene expression in several different cancer cell lines [16–20]. Moreover, FR901228 is known to increase viral and transgene expression following adenovirus infection [16]. These findings led us to examine whether FR901228 could augment the antitumor activity of OBP-301 against human cancer cells.

In the present study, we show that FR901228 treatment up-regulates CAR levels on target tumor cells, which in turn increases the amount of cellular viral replication, thereby promoting a synergistic antitumor effect. These findings suggest that treatment with OBP-301 in combination with FR901228 is a promising strategy for human cancer.

Results

Effect of FR901228 on CAR expression in human non-small cell lung cancer (NSCLC) cell lines

To explore the combination effect of OBP-301 and FR901228, we first used flow cytometry to determine if FR901228 has an effect on the cell surface expression of CAR. CAR was expressed in all four cell lines tested: the percentages of CAR-positive cells were 99.4%, 99.4%, 99.8%, and 86.8% in A549, H460, H358, and H1299 cells, respectively. As shown in Fig. 1A, CAR expression levels apparently increased in A549 and H460 cells following 48-h exposure to 1 ng/ml of FR901228, whereas H358 and H1299 cells showed a similar expression pattern of CAR before and after FR901228 treatment. The data were calculated as the relative mean fluorescent intensity (MFI), in which the MFI from FR901228-treated cells is divided by the MFI of cells without FR901228 treatment, thereby giving a fold enhancement of expression. In A549 and H460 cells, there were 1.6- and 2.15-fold higher MFI after FR901228 treatment compared to those before treatment, respectively (MFI: 61.13 to 97.88 [A549] and 59.51 to 127.94 [H460]). Western blot analysis for CAR expression also demonstrated that FR901228 treatment resulted in a 1.2-fold increase in the CAR protein level in A549 cells, whereas CAR protein expression level in H358 cells was consistent even after FR901228 treatment (Fig. 1B).

FR901228 has been previously reported to be a substrate for multidrug resistance protein (MDR1), which mediates FR901228 resistance in human cancer cells [21]. We next examined whether FR901228 treatment could alter MDR1 protein expression in the cell lines we used. As shown in Fig. 1C, MDR1 expression was not detected in these cell lines by Western blot analysis and could not be induced even after FR901228 treatment.

Adenovirus infectivity after FR901228 treatment in human NSCLC cell lines

To evaluate the effect of FR901228 on the infectious efficiency, we compared β-galactosidase-positive cells by X-gal staining 24 h after infection with recombinant replication-deficient adenovirus carrying the β-galactosidase gene under the control of cytomegalovirus (CMV) promoter (Ad-LacZ) in the presence or absence of FR901228. A549 and H1299 cells were treated with FR901228 at the indicated concentration for 48 h. Then, cells were infected with Ad-LacZ at multiplicities of infection (MOI) of 1 or 10 after removing medium containing FR901228. The X-gal staining 24 h after infection demonstrated that FR901228 treatment increased the percentage of blue-stained β-galactosidase-positive A549 cells in a dose-dependent manner; FR901228,

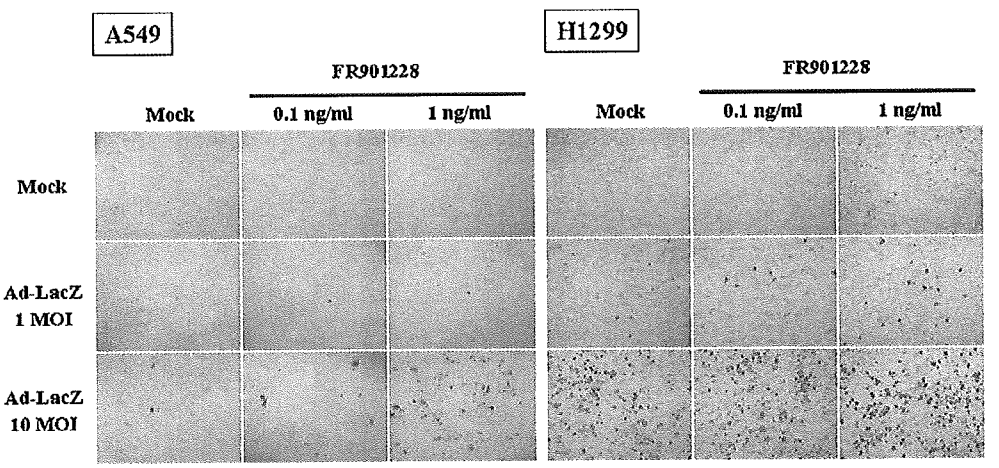

Fig. 2. Expression of β-galactosidase after Ad-LacZ infection in FR901228-treated cells. A549 and H1299 cells were treated with Ad-LacZ and FR901228 at the indicated concentrations, grown for 24 h, and then stained for β-galactosidase activity.

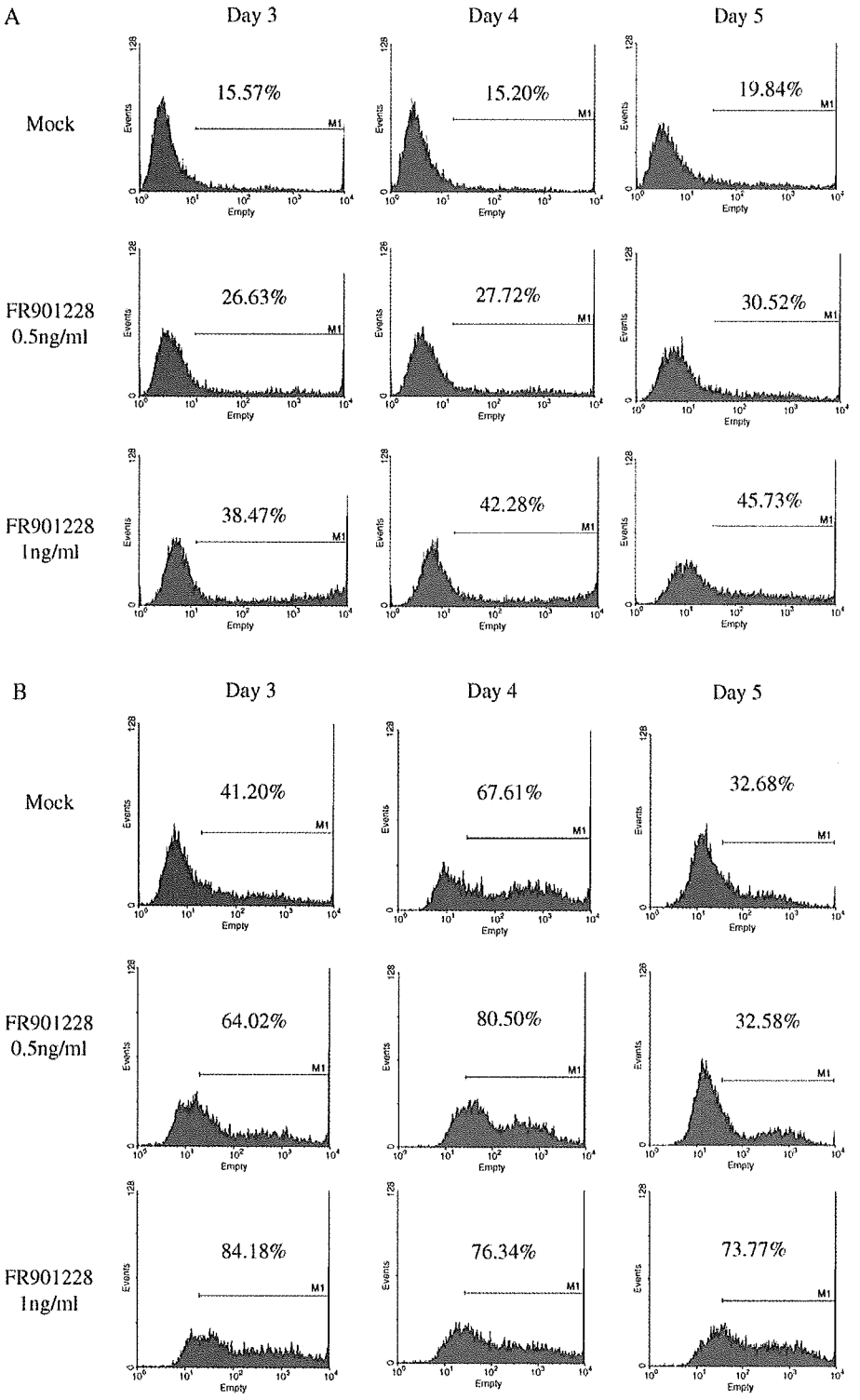

Fig. 3. Flow cytometric analysis of viral-replication-associated GFP expression following OBP-401 and FR901228 treatment. A549 (A), H460 (B), and H1299 (C) cells were infected with 0.1 MOI of OBP-401 and simultaneously treated with FR901228 at the indicated concentrations. The percentages of GFP-positive cells were assessed at different time points after treatment.

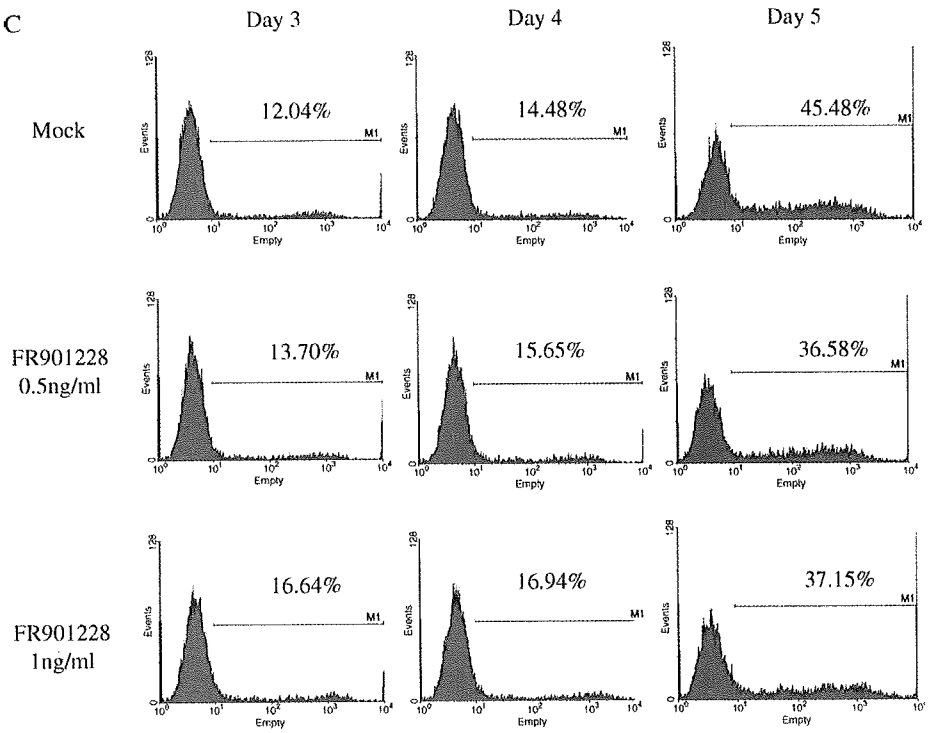

Fig. 3 (*continued*).

however, had no apparent effect on adenovirus infectious efficiency in H1299 cells (Fig. 2). These results were compatible with the effect of FR901228 treatment on CAR levels.

Oncolytic virus replication after FR901228 treatment in human NSCLC cell lines

We next examined the effect of FR901228 on oncolytic virus replication by flow cytometric analysis using telomerase-specific oncolytic adenovirus containing the GFP gene (OBP-401). The proportion of GFP-positive A549 cells increased from 15.57% (day 3) to 19.84% (day 5) after OBP-401 infection because OBP-401 can replicate in telomerase-positive tumor cells. However, the percentage of GFP-expressing cells was 45.73% in the presence of 1 ng/ml of FR901228 compared with 19.84% in cells without FR901228 at 5 days post-infection with 0.1 MOI of OBP-401 (Fig. 3A). Similarly, treatment with 1 ng/ml of FR901228 increased the percentage of GFP-expressing cells from 32.68% to 73.77% in H460 cells 5 days after infection with 0.1 MOI of OBP-401 (Fig. 3B). In contrast, there was no increase in the fraction of GFP-expressing cells after FR901228 treatment in H1299 cells (Fig. 3C). Moreover, the percentage of GFP-expressing H1299 cells decreased in the presence of 1 ng/ml of FR901228 5 days after OBP-401 infection, presumably due to the toxicity of FR901228.

To visualize viral replication in vitro, OBP-401-infected cells were photographed under a fluorescent microscope. As shown in Fig. 4, FR901228 increased the GFP fluorescence intensity in a dose-dependent manner on A549 and H460 cells 4 days after infection with 0.1 MOI of OBP-401. These findings are consistent with the results of flow

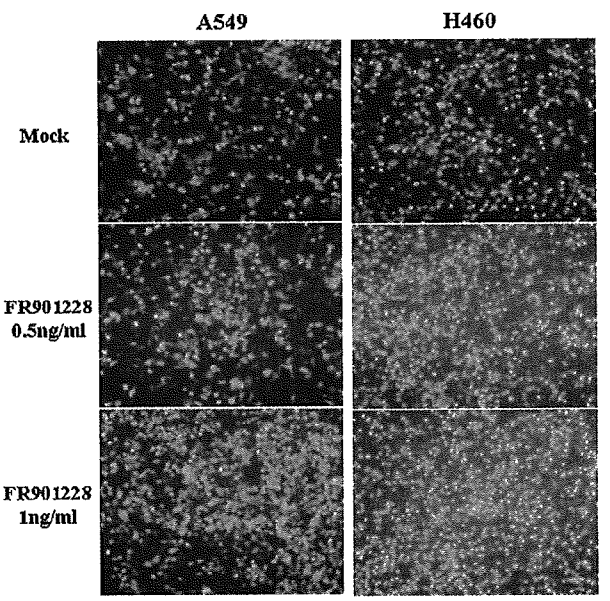

Fig. 4. Visualization of viral-replication-associated GFP expression following OBP-401 and FR901228 treatment. A549 and H460 cells were treated as described in the legend for Fig. 3. Cells were assessed for GFP expression with fluorescence microscopy 4 days after treatment.

cytometric analysis. The microphotographs also demonstrated that the number of GFP-positive cells increased in the presence of FR901228, indicating that OBP-401 could efficiently spread to the neighboring tumor cells. These results suggest that FR901228-induced up-regulation of CAR expression resulted in increased replication of oncolytic virus.

Cell cycle analysis after oncolytic virus infection and FR901228 treatment

To examine whether OBP-301 infection and FR901228 treatment result in cell cycle arrest, apoptosis, or a combination of both processes, the cell cycle distribution was determined by flow cytometric analysis of propidium-iodide-stained cells, a measure of DNA content. As shown in Table 1, neither OBP-301 infection nor FR901228 treatment affected the cell cycle distribution or the fraction of sub-G_0–G_1 apoptotic population in A549 and H460 cell lines.

Synergistic antitumor effect of OBP-301 and FR901228 in human NSCLC cells

We finally examined whether concurrent addition of FR901228 had an effect on the antitumor effect of OBP-301 in A549 cells. The cell viability with 8 doses of OBP-301 or 6 doses of FR901228 was assessed by MTT assay 4 days after treatment with concentrations that resulted in 0 to 100% cell kill when either drug was given alone (Fig. 5A). To determine whether the interaction between the two drugs exhibited synergistic cytotoxic effects, the data from the dose–response curves were examined by constructing isobolograms. Isobologram analysis indicated that the combination was synergistic across all dose levels tested, with all of the points lying into the area below the envelope of additivity (Fig. 5B). The combination index (CI) value of observed data points was 0.6823 ± 0.0761, which was smaller than 1. Thus, telomerase-specific oncolytic adenovirus OBP-301 in combination with FR901228 produces synergistic cell cytotoxicity in A549 human NSCLC cells.

Table 1
Cell cycle analysis after OBP-301 and FR901228 treatment

Cell line	Treatment	Sub-G_0/G_1 (%)	G_1 (%)	S (%)	G_2/M (%)
A549	Pre-treatment	2.04	68.74	15.35	14.18
	FR901228	1.13	74.58	10.43	13.88
	OBP-301	0.78	79.64	10.55	9.17
	FR901228 + OBP-301	2.24	73.08	11.58	13.26
H460	Pre-treatment	18.70	51.79	14.82	15.15
	FR901228	11.28	51.71	11.80	25.33
	OBP-301	1.07	69.70	14.72	14.56
	FR901228 + OBP-301	15.10	47.08	13.60	23.74

A549 and H460 cells were treated with 1 ng/ml of FR901228, 0.1 MOI of OBP-301, or both. The DNA content was determined by propidium iodide staining and flow cytometric analysis at 72 h after treatment. The percentage of cells in each stage of the cell cycle is shown.

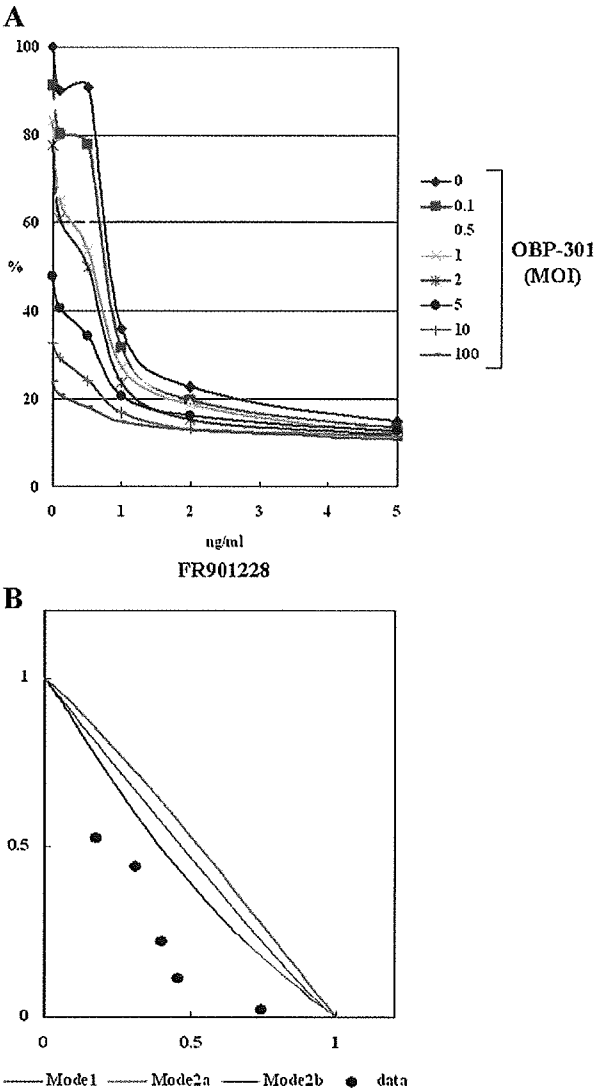

Fig. 5. Antitumor effect of OBP-301 and FR901228 on A549 NSCLC cells in vitro. (A) Effect of OBP-301 and FR901228 at various concentrations was assessed by MTT assay 4 days after treatment. Results are expressed as the percentage of untreated control. (B) The data from dose–response curves were subjected to isobologram analysis. Shown is the isobologram at IC50 based on the results of MTT assays for the A549 cell line treated with combinations of OBP-301 and FR901228 added simultaneously. Points below the envelope indicate a synergistic effect.

Discussion

Oncolytic adenovirus can efficiently kill a variety of human cancer cells; the death process, however, is morphologically distinct from apoptosis that is characterized by chromosome condensation and nuclear shrinkage and fragmentation [22]. In contrast, most of conventional chemotherapeutic drugs trigger apoptosis in human cancer

cells via caspase activation. These two types of anticancer agents that use different cytotoxic machinery have been shown to induce a combination effect [23–25], although the precise mechanism is still unclear. In an attempt to establish multidisciplinary therapeutics based on the rationale, we explored the antitumor effect of oncolytic virus in combination with an HDAC inhibitor. The HDAC inhibitor is a new class of anticancer agents that can modulate transcriptional activity [13,14]. As a result, in addition to the induction of apoptosis, HDAC inhibitors are able to block the cell cycle and angiogenesis, promote differentiation, and mediate additional unknown effects in human cancer cells. In the present study, we found that the most advanced therapeutic candidate, FR901228, had a synergistic antitumor effect with telomerase-specific oncolytic adenovirus OBP-301 through up-regulation of CAR expression in certain types of human NSCLC cells. This may be a novel therapeutic intervention of HDAC inhibitors.

Gene expression is considered to be regulated by chromatin remodeling. Chromatin is intrinsically modified by histone acetyltransferase or HDAC, and alterations in these mechanisms may lead to altered gene expression [26]. It has been reported that the activation of the CAR gene promoter is modulated by histone acetylation and that FR901228 increases CAR RNA levels through histone H3 acetylation in human cancer cells, leading to an increased adenovirus transgene expression [16–18]. Compatible with these observations, we demonstrated that FR901228 treatment led to increased levels of membrane-associated CAR protein in A549 and H460 human NSCLC cell lines (Figs. 1A, B). The reason why FR901228 did not affect CAR expression in H358 and H1299 cells is unclear. As all cell lines were negative for MDR1 expression that could mediate FR901228 resistance [21] (Fig. 1C), other mechanisms such as the Raf-MEK-ERK signal transduction pathway may be involved in CAR gene expression in H358 and H1299 cell lines [27].

We also confirmed increased infection efficiency of adenovirus following FR901228 treatment using Ad-LacZ vector (Fig. 2). One of the advantages of replication-competent oncolytic adenoviruses is that less virus particles are required for treatment because viruses can be produced in tumor tissues by replication. To directly evaluate the reliability of increased virus infectivity by FR901228 for oncolytic virus, we used Ad-LacZ at an MOI of 1 or 10, although 100 MOI of the vector was commonly used in previous studies. We previously reported that the fiber-modified oncolytic adenovirus (OBP-405) containing an RGD motif in the HI loop of the fiber knob showed increased initial virus entry into the target tumor cells and resulted in the augmented viral replication [10]. Thus, FR901228 treatment is expected to enhance virus infectivity as well as replication in A549 and H460 cells. In fact, the percentages of GFP-positive cells were more than 2-fold higher in A549 and H460 cells treated with GFP-expressing OBP-401 in combination with FR901228 than those infected with OBP-401 alone (Figs. 3 and 4). Studies using a non-viral plasmid vector have found that FR901228 enhances luciferase transgene expression at the transcriptional level [28]. Therefore, it is possible that increased GFP expression reflects transcriptionally enhanced transgene expression, but not viral replication. However, the fact that FR901228 treatment did not affect OBP-401-induced GFP expression in H1299 cells suggests that FR901228 could not alter the levels of transgene expression without CAR up-regulation and that GFP expression is dependent on virus infectivity and replication. Taken together, FR901228 increases CAR expression, which in turn facilitates virus infection, thereby leading to increased viral replication in certain types of human NSCLC cells.

Adenovirus replication within a target tumor cell can cause cell destruction by several mechanisms such as direct cytotoxicity due to viral proteins and augmentation of antitumoral immunity [2]. As expected, OBP-301 in combination with FR901228 demonstrated a profound antitumor effect in vitro in A549 cells, presumably because of enhanced viral replication. Isobologram and CI analyses, which are the two most popular methods for evaluating drug interactions in combination cancer chemotherapy [29], consistently identified OBP-301 infection and FR901228 treatment as a synergistic combination (Fig. 5). Theoretically, some chemotherapeutic drugs could act to inhibit viral replication because they might affect the cell cycle; our data, however, demonstrated that FR901228 with or without OBP-301 had no effect on the cell cycle distribution (Table 1), indicating that FR901228 may be an appropriate partner for oncolytic adenovirus because it does not affect the virus life cycle. Moreover, phase I clinical trials for advanced cancer as well as leukemia have shown that FR901228 can be safely administered without any life-threatening toxicities or cardiac toxicities, although the appropriate administration schedule has to be further examined [30,31]. These observations indicate that clinical trials of OBP-301 in combination with FR901228 are warranted.

In conclusion, our data demonstrate a possible interaction between a telomerase-specific oncolytic adenoviral agent and an HDAC inhibitor. Delineating specific virus/drug combinations that are tailored to be particularly effective in human cancer may have the potential to greatly improve the already encouraging results seen in the field of oncolytic virotherapy.

Materials and methods

Cells and culture conditions

The NSCLC cell lines A549, H460, H358, and H1299 were propagated in monolayer culture in RPMI 1640 medium supplemented with 10% fetal calf serum, 25 mM HEPES, 100 units/ml penicillin, and 100 μg/ml streptomycin.

Compounds

FR901228 was kindly provided by the Fujisawa Pharmaceutical Company (Tokyo, Japan).

Recombinant adenoviruses

The recombinant replication-selective, tumor-specific adenovirus vector OBP-301 (Telomelysin) was previously constructed and characterized [7,32]. Replication-selective OBP-401 (Telomelysin-GFP) containing GFP cDNA under the control of the CMV promoter and replication-deficient adenoviral vector containing β-galactosidase cDNA (Ad-LacZ) were also used [33]. These viruses were purified by $CsCl_2$ step gradient ultracentrifugation followed by $CsCl_2$ linear gradient ultracentrifugation. Determination of virus particle titer and infectious titer was accomplished spectrophotometrically by the method of Maizel et al. [34] and by the method of Kanegae et al. [35], respectively.

Flow cytometry

The cells (2×10^5 cells) were labeled with mouse monoclonal anti-CAR (RmcB; Upstate Biotechnology, NY) for 30 min at 4°C, incubated with FITC-conjugated rabbit anti-mouse IgG second antibody (Zymed Laboratories, San Francisco), and analyzed by the FACSCalibur (Becton Dickinson, Mountain View, CA) using CELL Quest software. The window was set to exclude dead cells and debris. Expression of the GFP gene was also assessed by the FACSCalibur.

Western blot analysis

The primary antibodies against CAR (RmcB; Upstate Biotechnology) and MDR1 (DAKO, Carpinteria, CA) and peroxidase-linked secondary antibody (Amersham, Arlington Heights, IL) were used. Cells were washed twice in cold PBS and collected then lysed in lysis buffer [10 mM Tris (pH 7.5), 150 mM NaCl, 50 mM NaF, 1 mM EDTA, 10% glycerol, 0.5% NP40] containing proteinase inhibitors (0.1 mM phenylmethylsulfonyl fluoride, 0.5 mM Na_3VO_4). After 20 min on ice, the lysates were spun at 14,000 rpm in a microcentrifuge at 4°C for 10 min. The supernatants were used as whole cell extracts. Protein concentration was determined using the Bio-Rad protein determination method (Bio-Rad, Richmond, CA). Equal amounts (50 μg) of proteins were boiled for 5 min and electrophoresed under reducing conditions on 6–12.5% (w/v) polyacrylamide gels. Proteins were electrophoretically transferred to a Hybond-polyvinylidene difluoride (PVDF) transfer membranes (Amersham Life Science, Buckinghamshire, UK) and incubated with the primary followed by peroxidase-linked secondary antibody. An Amersham ECL chemiluminescent western system (Amersham) was used to detect secondary probes.

X-gal staining

Cells were seeded in 6-well plates (2×10^5 cells/well) and infected with Ad-LacZ at indicated MOIs. X-gal (5-bromo-4-chloro-3-indolyl-β-D-galactopyranoside) staining was performed 24 h after infection according to the protocol provided by the manufacturer (Sigma-Aldrich, St. Louis, MO).

MTT assay, isobologram analysis, and CI analysis

The cytotoxicity of FR901228 and OBP-301 was determined by measurement of cell viability by using the 3-(4,5-dimethylthiazol-2-yl)-2,5-diphenyltetrazolium bromide (MTT) assay. Cells were plated in 96-well tissue culture plates 24 h before treatment. Then, cells were treated with FR901228 and OBP-301 concurrently at the indicated concentrations and MOIs, respectively. Four days later, a medium containing 0.5 mg/ml MTT (Sigma) was added to each well after the wells were rinsed with PBS. After a 4-h incubation at 37°C, an equal amount of solubilization solution (0.04 N HCl in isopropyl alcohol) was added to each well and mixed thoroughly to dissolve the crystals of MTT formazan. Results were quantified using a Labsystems Multiskan MS at 540 nm wave length. Control absorbance was designated as 100%, and cell survival was expressed as a percentage of control absorbance. MTT results were analyzed quantitatively and statistically by plotting the observed experimental data onto the isobologram [29]. When the observed data points for a combination fell mainly within the envelope of additivity, the effect of the combination was considered as having an additive effect. When the observed data points for a combination fell into the area below the envelope of additivity, the combination effect was regarded as supra-additive (synergism). When the observed data points for a combination fell above the envelope but within the square or the cube, the combination's effect was considered as sub-additive. When the observed data points for a combination fell outside the square or the cube, the effect of the combination was considered protective. Both sub-additive and protective interactions were considered as antagonistic. CI analysis, similar to isobologram analysis, provides qualitative information on the nature of drug interaction. CI is a numerical value calculated as described previously. CIs of less than, equal to, and more than 1 indicate synergy, additivity, and antagonism, respectively. All of the analyses were performed using Statistica software (StatSoft Inc., Tulsa, Oklahoma).

Acknowledgments

We thank the Fujisawa Pharmaceutical Company for providing FR901228. We thank Yoshiko Shirakiya, Yuuri Hashimoto, and Nobue Mukai for their excellent technical

assistance. This work was supported in part by grants from the Ministry of Education, Science, and Culture, Japan and grants from the Ministry of Health and Welfare, Japan.

References

[1] L.K. Hawkins, N.R. Lemoine, D. Kirn, Oncolytic biotherapy: a novel therapeutic platform, Lancet Oncol. 3 (2002) 17–26.
[2] E.A. Chiocca, Oncolytic viruses, Nat. Rev., Cancer 2 (2002) 938–950.
[3] J. Nemunaitis, F. Khuri, I. Ganly, J. Arseneau, M. Posner, E. Vokes, J. Kuhn, T. McCarty, S. Landers, A. Blackburn, L. Romel, B. Randlev, S. Kaye, D. Kirn, Phase II trial of intratumoral administration of ONYX-015, a replication-selective adenovirus, in patients with refractory head and neck cancer, J. Clin. Oncol. 19 (2001) 289–298.
[4] T.L. DeWeese, H. van der Poel, S. Li, B. Mikhak, R. Drew, M. Goemann, U. Hamper, R. DeJong, N. Detorie, R. Rodriguez, T. Haulk, A.M DeMarzo, S. Piantadosi, D.C. Yu, Y. Chen, D.R. Henderson, M.A. Carducci, W.G. Nelson, J.W. Simons, A phase I trial of CV706, a replication-competent, PSA selective oncolytic adenovirus, for the treatment of locally recurrent prostate cancer following radiation therapy, Cancer Res. 61 (2001) 7464–7472.
[5] T. Reid, E. Galanis, J. Abbruzzese, D. Sze, L.M. Wein, J. Andrews, B. Randlev, C. Heise, M. Uprichard, M. Hatfield, L. Rome, J. Rubin, D. Kirn, Hepatic arterial infusion of a replication-selective oncolytic adenovirus (dl1520): phase II viral, immunologic, and clinical endpoints, Cancer Res. 62 (2002) 6070–6079.
[6] O. Hamid, M.L. Varterasian, S. Wadler, J.R. Hecht, A. Benson, E. Galanis, M. Uprichard, C. Omer, P. Bycott, R.C. Hackman, A.F. Shields, Phase II trial of intravenous CI-1042 in patients with metastatic colorectal cancer, J. Clin. Oncol. 21 (2003) 1498–1504.
[7] T. Kawashima, S. Kagawa, N. Kobayashi, Y. Shirakiya, T. Umeoka, F. Teraishi, M. Taki, S. Kyo, N. Tanaka, T. Fujiwara, Telomerase-specific replication-selective virotherapy for human cancer, Clin. Cancer Res. 10 (2004) 285–292.
[8] J.M. Bergelson, J.A. Cunningham, G. Droguett, E.A. Kurt-Jones, A. Krithivas, J.S. Hong, M.S. Horwitz, R.L. Crowell, R.W. Finberg, Isolation of a common receptor for Coxsackie B viruses and adenoviruses 2 and 5, Science 275 (1997) 1320–1323.
[9] R.P. Tomko, R. Xu, L. Philipson, HCAR and MCAR: the human and mouse cellular receptors for subgroup C adenoviruses and group B coxsackieviruses, Proc. Natl. Acad. Sci. U. S. A. 94 (1997) 3352–3356.
[10] M. Taki, S. Kagawa, M. Nishizaki, H. Mizuguchi, T. Hayakawa, S. Kyo, K. Nagai, Y. Urata, N. Tanaka, T. Fujiwara, Enhanced oncolysis by a tropism-modified telomerase-specific replication-selective adenoviral agent OBP-405 ('Telomelysin-RGD'), Oncogene 24 (2005) 3130–3140.
[11] H. Mizuguchi, T. Hayakawa, Enhanced antitumor effect and reduced vector dissemination with fiber-modified adenovirus vectors expressing herpes simplex virus thymidine kinase, Cancer Gene Ther. 9 (2002) 236–242.
[12] A.V. Borovjagin, A. Krendelchtchikov, N. Ramesh, D.C. Yu, T.J. Douglas, D.T. Curiel, Complex mosaicism is a novel approach to infectivity enhancement of adenovirus type 5-based vectors, Cancer Gene Ther. 12 (2005) 475–486.
[13] H. Ueda, H. Nakajima, Y. Hori, T. Fujita, M. Nishimura, T. Goto, M. Okuhara, FR901228, a novel antitumor bicyclic depsipeptide produced by *Chromobacterium violaceum* No. 968: I. Taxonomy, fermentation, isolation, physico-chemical and biological properties, and antitumor activity, J. Antibiot. (Tokyo) 47 (1994) 301–310.
[14] H. Nakajima, Y.B. Kim, H. Terano, M. Yoshida, S. Horinouchi, FR901228, a potent antitumor antibiotic, is a novel histone deacetylase inhibitor, Exp. Cell Res. 241 (1998) 126–133.
[15] R. Furumai, A. Matsuyama, N. Kobashi, K.H. Lee, M. Nishiyama, H. Nakajima, A. Tanaka, Y. Komatsu, N. Nishino, M. Yoshida, S. Horinouchi, FK228 (depsipeptide) as a natural prodrug that inhibits class I histone deacetylases, Cancer Res. 62 (2002) 4916–4921.
[16] M. Kitazono, M.E. Goldsmith, T. Aikou, S. Bate, T. Fojo, Enhanced adenovirus transgene expression in malignant cells treated with the histone deacetylase inhibitor FR901228, Cancer Res. 61 (2001) 6230–6328.
[17] M. Kitazono, V.K. Rao, R. Robey, T. Aikou, S. Bates, T. Fojo, M.E. Goldsmith, Histone deacetylase inhibitor FR901228 enhances adenovirus infection of hematopoietic cells, Blood 99 (2002) 2248–2251.
[18] M.E. Goldsmit, M. Kitazono, P. Fok, T. Aikou, S. Bates, T. Fojo, The histone deacetylase inhibitor FK228 preferentially enhances adenovirus transgene expression in malignant cells, Clin. Cancer Res. 9 (2003) 5394–5401.
[19] R.C. Pong, Y.J. Lai, H. Chen, T. Okegawa, E. Frenkel, A. Sagalowsky, J.T. Hsieh, Epigenetic regulation of coxsackie and adenovirus receptor (CAR) gene promoter in urogenital cancer cells, Cancer Res. 63 (2003) 8680–8686.
[20] A. Hemminki, A. Kanerva, B. Liu, M. Wang, R.D. Alvarez, G.P. Siegal, D.T. Curiel, Modulation of coxsackie-adenovirus receptor expression for increased adenoviral transgene expression, Cancer Res. 63 (2003) 847–853.
[21] J.J. Xiao, Y. Huang, Z. Dai, W. Sadee, J. Chen, S. Liu, G. Marcucci, J. Byrd, J.M. Covey, J. Wright, M. Grever, K.K. Chan, Chemoresistance to depsipeptide FK228 [(*E*)-(1*S*,4*S*,10*S*,21*R*)-7-[(*Z*)-ethylidene]-4,21-diisopropyl-2-oxa-12,13-dithia-5,8,20,23-tetraazabicyclo[8,7,6]-tricos-16-ene-3,6,9,22-pentanone] is mediated by reversible MDR1 induction in human cancer cell lines, J. Pharmacol. Exp. Ther. 314 (2005) 467–475.
[22] E.I. Abou, M.A. Hassan, I. van der Meulen-Muileman, S. Abbas, F.A. Kruyt, Conditionally replicating adenoviruses kill tumor cells via a basic apoptotic machinery-independent mechanism that resembles necrosis-like programmed cell death, J. Virol. 78 (2004) 12243–12251.
[23] C. Heise, A. Sampson-Johannes, A. Williams, F. McCormick, D.D. Von Hoff, D.H. Kirn, ONYX-015, an E1B gene-attenuated adenovirus, causes tumor-specific cytolysis and antitumoral efficacy that can be augmented by standard chemotherapeutic agents, Nat. Med. 3 (1997) 639–645.
[24] D.C. Yu, Y. Chen, J. Dilley, Y. Li, M. Embry, H. Zhang, N. Nguyen, P. Amin, J. Oh, D.R. Henderson, Antitumor synergy of CV787, a prostate cancer-specific adenovirus, and paclitaxel and docetaxel, Cancer Res. 61 (2001) 517–525.
[25] J. Zhang, N. Ramesh, Y. Chen, Y. Li, J. Dilley, P. Working, D.C. Yu, Identification of human uroplakin II promoter and its use in the construction of CG8840, a urothelium-specific adenovirus variant that eliminates established bladder tumors in combination with docetaxel, Cancer Res. 62 (2002) 3743–3750.
[26] G.J. Narlikar, H.Y. Fan, E.C. Kingston, Cooperation between complexes that regulate chromatin structure and transcription, Cell 108 (2002) 475–487.
[27] M. Anders, C. Christian, M. McMahon, F. McCormick, W.M. Korn, Inhibition of the Raf/MEK/ERK pathway up-regulates expression of the coxsackievirus and adenovirus receptor in cancer cells, Cancer Res. 63 (2003) 2088–2095.
[28] T. Yamano, K. Ura, R. Morishita, H. Nakajima, M. Monden, Y. Kaneda, Amplification of transgene expression in vitro and in vivo using a novel inhibitor of histone deacetylase, Mol. Ther. 1 (2000) 574–580.
[29] M. Nishizaki, R.E. Meyn, L.B. Levy, E.N. Atkinson, R.A. White, J.A. Roth, L. Ji, Synergistic inhibition of human lung cancer cell growth by adenovirus-mediated wild-type p53 gene transfer in combination with docetaxel and radiation therapeutics in vitro and in vivo, Clin. Cancer Res. 7 (2001) 2887–2897.

[30] J.L. Marshall, N. Rizvi, J. Kauh, W. Dahut, M. Figuera, M.H. Kang, W.D. Figg, I. Wainer, C. Chaissang, M.Z. Li, M.J. Hawkins, A phase I trial of depsipeptide (FR901228) in patients with advanced cancer, J. Exp. Ther. Oncol. 2 (2002) 325–332.

[31] J.C. Byrd, G. Marcucci, M.R. Parthun, J.J. Xiao, R.B. Klisovic, M. Moran, T.S. Lin, S. Liu, A.R. Sklenar, M.E. Davis, D.M. Lucas, B. Fischer, R. Shank, S.L. Tejaswi, P. Binkley, J. Wright, K.K. Chan, M.R. Grever, A phase I and pharmacodynamic study of depsipeptide (FK228) in chronic lymphocytic leukemia and acute myeloid leukemia, Blood 105 (2005) 959–967.

[32] T. Umeoka, T. Kawashima, S. Kagawa, F. Teraishi, M. Taki, M. Nishizaki, S. Kyo, K. Nagai, Y. Urata, N. Tanaka, T. Fujiwara, Visualization of intrathoracically disseminated solid tumors in mice with optical imaging by telomerase-specific amplification of a transferred green fluorescent protein gene, Cancer Res. 64 (2004) 6259–6265.

[33] Y. Tango, M. Taki, Y. Shirakiya, S. Ohtani, N. Tokunaga, Y. Tsunemitsu, S. Kagawa, T. Tani, N. Tanaka, T. Fujiwara, Late resistance to adenoviral p53-mediated apoptosis caused by decreased expression of Coxsackie-adenovirus receptors in human lung cancer cells, Cancer Sci. 95 (2004) 459–463.

[34] J.V.J. Maizel, D.O. White, M.D. Scharff, The polypeptides of adenovirus: I. Evidence for multiple protein components in the virion and a comparison of types 2, 7A, and 12, Virology 36 (1968) 115–125.

[35] Y. Kanegae, M. Makimura, I. Saito, A simple and efficient method for purification of infectious recombinant adenovirus, Jpn. J. Med. Sci. Biol. 47 (1994) 157–166.

TECHNICAL REPORTS

In vivo imaging of lymph node metastasis with telomerase-specific replication-selective adenovirus

Hiroyuki Kishimoto[1,2], Toru Kojima[1,2], Yuichi Watanabe[1,3], Shunsuke Kagawa[1,2], Toshiya Fujiwara[1,2], Futoshi Uno[1,2], Fuminori Teraishi[1,2], Satoru Kyo[4], Hiroyuki Mizuguchi[5], Yururi Hashimoto[3], Yasuo Urata[3], Noriaki Tanaka[1],& Toshiyoshi Fujiwara[1,2]

[1]Division of Surgical Oncology, Department of Surgery, Okayama University Graduate School of Medicine, Dentistry and Pharmaceutical Sciences, 2-5-1 Shikata-cho, Okayama 700-8558, Japan. [2]Center for Gene and Cell Therapy, Okayama University Hospital, 2-5-1 Shikata-cho, Okayama 700-8558, Japan. [3]Oncolys BioPharma, Inc., 2-3-9 Roppongi, Minato-ku, Tokyo 106-0032, Japan. [4]Department of Obstetrics and Gynecology, Kanazawa University School of Medicine, 13-1 Takara-machi, Kanazawa 920-8641, Japan. [5]Laboratory of Gene Transfer and Regulation, National Institute of Biomedical Innovation, 7-6-8 Saito-Asagi, Ibaraki, Osaka 567-0085, Japan.

Correspondence should be addressed to T. F. (toshi_f@md.okayama-u.ac.jp).

Abstract

Currently available methods for detection of tumors *in vivo* such as computed tomography and magnetic resonance imaging are not specific for tumors. Here we describe a new approach for visualizing tumors whose fluorescence can be detected using telomerase-specific replication-competent adenovirus expressing green fluorescent protein (GFP) (OBP-401). OBP-401 contains the replication cassette, in which the human telomerase reverse transcriptase (hTERT) promoter drives expression of *E1* genes, and the *GFP* gene for monitoring viral replication. When OBP-401 was intratumorally injected into HT29 tumors orthotopically implanted into the rectum in BALB/c *nu/nu* mice, para-aortic lymph node metastasis could be visualized at laparotomy under a three-chip color cooled charged-coupled device camera. Our results indicate that OBP-401 causes viral spread into the regional lymphatic area and selectively replicates in neoplastic lesions, resulting in GFP expression in metastatic lymph nodes. This technology is adaptable to detect lymph node metastasis *in vivo* as a preclinical model of surgical navigation.

Medical imaging techniques have become an essential aspect of cancer diagnosis, detection, and treatment monitoring. Advances and improvements in the major imaging modalities such as computed tomography (CT), magnetic resonance imaging (MRI), and ultrasound techniques have increased the sensitivity of visualizing tumors and their metastases in the body[1, 2]. A limiting factor of these techniques is, however, the inability to specifically identify malignant tissues. Positron emission tomography (PET), with the glucose analogue ^{18}F-2-deoxy-D-glucose (FDG), is the first molecular imaging technique that has been widely applied for cancer imaging in clinical settings[3]. Although FDG-PET has high detection sensitivity, it has some limitations such as the difficulty in distinguishing between proliferating tumor cells and inflammation and the inability to be used for real-time detection of tumor tissues. A relatively inexpensive, robust, and straightforward way of defining the location and area of tumors *in vivo* would greatly aid the treatment of human cancer, especially for surgical procedures. In particular, if tumors too small for direct visual detection and therefore not detectable by direct inspection could be imaged *in situ*, surgeons could excise such tumors precisely with appropriate surgical margins.

Sentinel lymph node (SLN) mapping is a minimally invasive procedure and widely used in the management of patients with cutaneous melanoma or breast cancer without clinical evidence of nodal metastases[4, 5]. The technique assumes that early lymphatic metastases, if present, are always found first within the SLN, the first tumor-draining lymph node. A SLN free of tumor cells would therefore predict the

absence of metastatic disease in the rest of the tumor-draining lymph node basin, which indicates that intensive lymphadenectomy is unlikely to benefit those patients. Several studies have validated this assumption; the sensitivity of intraoperative frozen-section analysis for detection of nodal metastases, however, is relatively low and high false-negative rates have been reported[6-9]. In addition, thicker primary and larger SLN tumor size has been shown to be predictive of non-SLN metastasis, presumably because of the altered lymphatic drainage routes. These findings raise doubt about the applicability of this technique in widespread surgical practice and, therefore, a number of approaches have been taken to directly label tumor cells to visualize and track them *in vivo*.

The green fluorescent protein (GFP), which was originally identified from the jellyfish *Aequorea Victoria*, is an attractive molecular marker for imaging in live tissues because of the relatively non-invasive nature of fluorescent[10-15]. We previously demonstrated a real-time fluorescence optical imaging of pleural dissemination of human non-small cell lung cancer cells in an orthotopic mouse model using tumor-specific replication-competent adenovirus (OBP-301, Telomelysin)[16, 17] in combination with replication-deficient adenovirus expressing *GFP* (Ad-*GFP*)[18]. In the present study, we further modified OBP-301 to contain the *GFP* gene driven by the cytomegalovirus (CMV) promoter for monitoring viral replication. The resultant adenovirus, termed OBP-401, efficiently labeled tumor cells with green fluorescence *in vitro* and *in vivo*. The results showed that injection of OBP-401 into primary tumors

allows its lymphatic spread, which in turn induces viral replication in metastatic lymph nodes, thereby leading to the direct imaging of micrometastases. This technology is adaptable to detect lymph node metastasis *in vivo* as a preclinical model of surgical navigation.

RESULTS

hTERT levels in human cell lines and lymph node metastases

To confirm the specificity of telomerase activity in human cancer cells, we measured expression of *hTERT* mRNA in a panel of human tumor and normal cell lines using a real-time reverse transcription (RT)-PCR method. Although the levels of expression varied widely, all tumor cell lines derived from different organs expressed detectable levels of *hTERT* mRNA, whereas human fibroblast cells such as NHLF and WI38, human vascular endothelial cells (HUVEC), and normal human renal epithelial cells (HRE) were negative for *hTERT* expression (**Fig. 1a**). We also examined samples of 30 primary tumors and 39 lymph node metastases obtained form gastric cancer patients for hTERT protein expression by immunohistochemistry (**Supplementary Table 1** online). As shown in **Fig. 1b**, hTERT staining was clearly observed in metastatic foci of gastric cancers, although most of lymphocytes present in lymph nodes were hTERT-negative except in some germinal centers. These results suggest that the hTERT promoter element can be used to target human cancer.

Selective visualization of human cancer cells *in vitro*

We constructed the tumor-specific replication-competent adenovirus OBP-401 that expresses *GFP* by inserting the *GFP* gene under the control of the CMV promoter at the deleted E3 region of the telomerase-specific replication selective type 5 adenovirus OBP-301[16, 17] (**Fig. 1c**). To evaluate the replication ability of OBP-401 in different cell lines, we measured the relative amounts of *E1A* DNA by quantitative real-time PCR analysis. Human cancer cells (H1299 and SW620) and normal cells (NHLF) were infected with OBP-401 at an MOI of 10 for 2 h, followed by incubation in the medium. Cells were harvested at various times over 3 d after infection, and the virus yield was determined by quantitative real-time PCR assay targeting for the viral *E1A* sequence. The ratios were normalized by dividing the value of cells obtained 2 h after viral infection. In SW620 and H1299 cells, OBP-401 replicated 6-7 logs by 3 d after infection; OBP-401 replication, however, was attenuated up to 3 logs in normal NHLF cells (**Fig. 1d**). These findings indicate that OBP-401 viral recovery was reduced by 3-4 logs in normal cells compared with cancer cells. We also found an apparent correlation between viral yields at 24 h after OBP-401 infection and *hTERT* mRNA expression levels in human cancer cell lines (**Fig. 1e**).

To determine whether OBP-401 replication is associated with selective GFP expression, cells were analyzed and photographed by fluorescent microscope after OBP-401 infection. As shown in **Fig. 2a**, H1299 human non-small cell lung cancer

cells expressed bright GFP fluorescence as early as 12 h after OBP-401 infection at an MOI of 10. The fluorescence intensity gradually increased in a dose-dependent fashion until approximately 72 h after infection, followed by rapid cell death due to the cytopathic effect of OBP-401, as evidenced by floating, highly light-refractile cells under phase-contrast photomicrographs. In SW620 and HT29 human colorectal cancer cells, we detected GFP expression 24 h after infection with 10 MOI of OBP-401, and cells showed the cytopathic effect at 72 h post-infection (**Fig. 2b, c**). In contrast, normal NHLF cells were negative for GFP expression after OBP-401 infection (**Fig. 2d**). These results indicate that OBP-401 can replicate exclusively in human cancer cells, leading to tumor cell-specific GFP fluorescence expression *in vitro*. We detected replicating virus particles in human cancer cells by transmission electron microscopy (**Fig. 2e**). The cytopathic effect of OBP-401 was also assessed by the XTT cell viability assay. In both SW620 and HT29 cells, OBP-401 infection induced rapid cell death in a dose-dependent manner (**Supplementary Fig. 1a** online). In *nu/nu* mice carrying subcutaneous SW620 human colorectal tumor xenografts, intratumoral injection of OBP-401 resulted in a significant inhibition of tumor growth compared with mock-treated tumors (**Supplementary Fig. 1b** online).

Selective visualization of subcutaneous tumors *in vivo*

It is reported that the hTERT promoter could be used to induce transgene expression in syngenic tumors in mice[19]. We first confirmed that OBP-401 could replicate and

express GFP fluorescence in Colon-26 cells *in vitro* as well as *in vivo* (**Supplementary Fig. 2a, b** online). In contrast, OBP-401 replication was attenuated in mouse splenocytes (**Supplementary Fig. 2a** online). These results suggest that the hTERT promoter can efficiently use the mouse transcriptional machinery and, therefore, the selectivity of OBP-401 can be examined in human tumor xenografts in mice.

To assess the specificity of the GFP-based fluorescent optical detection of tumors *in vivo*, we examined the kinetics of GFP transgene expression in subcutaneous SW620 and HT29 tumors after intratumoral injection of 1×10^7 PFU/100 μl of OBP-401 with the CCD non-invasive imaging system. Whole-body images of mice showed that intratumoral GFP fluorescence signals were detectable within 24 h after local delivery of viruses (**Fig. 3a**). The fluorescence intensity reached maximum levels within 4 d post-injection, and was maintained for at least 7 d. When SW620 tumors were removed 14 d after intratumoral injection of OBP-401, the high GFP transgene expression was visible on the surface of tumors as well as across serially-sliced sections (**Fig. 3b**). No GFP fluorescence was detected when non-tumor-bearing mice were subcutaneously injected with 1×10^7 PFU/100 μl of OBP-401 (**Fig. 3c**), suggesting confinement of GFP expression to the tumor.

Orthotopic mouse model of human rectal cancer with metastasis

The development of the orthotopic implantation technique for human rectal cancer has

been described previously[20]. Our preliminary experiments revealed that, when 5 x 10^6 HT29 human colorectal cancer cells suspended in Matrigel are inoculated into the rectum submucosa of athymic *nu/nu* mice, rectal tumors appeared within 7 d after tumor injection (**Fig. 4a, b**). Histopathological examination of the excised primary tumor showed a submucosal tumor formation composed of implanted HT29 cells with a solid architecture and invasion into the muscularis propria and submucosa (**Fig. 4c**). Examination under high magnification showed tumor cell-filled lymphatic vessels in the muscularis propria layer (**Fig. 4c**). As expected, we detected the green fluorescence expression from 24 h after intratumoral administration of OBP-401 in the primary rectal tumors with maximum signal occurring 2 to 4 d post-injection, whereas tumors not injected with OBP-401 were completely GFP-negative (**Fig. 4d**).

Selective visualization of lymph node metastasis

In our preliminary experiments, we confirmed that most mice with rectal tumors subsequently developed lymph node metastasis around the abdominal aorta from the lower margin of the renal vein to the aortic bifurcation, which were microscopically detectable approximately 4 weeks after tumor inoculation. Five days after injection of 1×10^8 PFU of OBP-401 into the implanted rectal tumors, we explored the abdominal cavity at laparotomy. Analyses of two representative mice are shown in **Fig. 4**. Three lymph nodes (LN1, LN2, and LN3) were macroscopically identified adjacent to the aorta (**Fig. 4e, f**); the optical CCD imaging of the abdominal cavity, however,

demonstrated that only one lymph node (LN3) could be detected as light emitting spots with GFP fluorescence (**Fig. 4f**). In the other mouse, 3 of 4 lymph nodes could be imaged as GFP signals (**Fig. 4h**). We detected no GFP fluorescence in abdominal lymph nodes after injection of 1×10^7 PFU of OBP-401 into the rectal tumors (data not shown). Histopathological analysis confirmed the presence of metastatic adenocarcinoma cells in the lymph nodes with fluorescence emission, whereas GFP-negative lymph nodes contained no tumor cells (**Fig. 4g, i**). In addition, immunohistochemical analysis for GFP protein demonstrated that the reddish-brown GFP-immunoreactive cells corresponded to the microscopic metastatic nodules in the lymph nodes, but were not detected in the non-metastatic lymphocyte area (**Supplementary Fig. 3** online).

We verified the GFP-based fluorescence detection with OBP-401 and histological correlation of lymph node metastasis in a series of *in vivo* experiments. Representative examples of the data are summarized in **Table 1**. Among the 7 tumor-bearing mice, 6 mice (85.7%) developed histologically confirmed lymph node metastasis. Of 28 lymph nodes excised from 7 mice, histopathological analysis demonstrated that 13 nodes (46.4%) contained micrometastatic nodules. The optical CCD imaging detected 12 lymph nodes labeled in spots with GFP fluorescence in 13 metastatic nodes (sensitivity of 92.3%). Among 15 metastasis-free lymph nodes, 2 nodes were GFP-positive (specificity of 86.6%). Our results indicate that intratumoral injection of OBP-401 causes viral spread into the regional lymphatic area and selective